NUCL SCI TECH (2017) 28:23
DOI 10.1007/s41365-016-0176-5

A new method for position-sensitive measurement of beta surface contamination

Yan-Tao Qu[1] · Hui Wang[1] · Yang Liu[1] · Ling Chen[1] · Jie Hou[2] · Zhe Liu[1] · Ji-Zeng Ma[1,3]

Received: 26 April 2015 / Revised: 4 September 2015 / Accepted: 6 September 2015 / Published online: 26 December 2016

Abstract In this paper, we propose a new method for position-sensitive measurement of beta surface contamination. With a position-sensitive detector of enlarged sensitive detection area, accurate information of the contamination distribution can be obtained. The position-sensitive detection is based on a large-area plastic scintillator and the wavelength shifting (WLS) fibers and adopts the "light center of gravity" method. Optical transmission of the detector is simulated with a preliminary detector model, and feasibility of the detector design and measurement method is evaluated using an experiment system. The simulation and experiment results at different beta-ray incident points on the scintillator surface show that there is a polynomial relationship between the average amplitude ratio of the output pulses from the two parallel WLS fibers in the same fiber layer and the relative distance from the incident point to the WLS fiber.

Keywords Beta surface contamination · Position-sensitive measurement · Wavelength shifting fibers · Plastic scintillator

This work was supported by the Technology and Industry for National Defense (No. HK.FA1001-1).

✉ Yan-Tao Qu
quyantao19820831@126.com

1 Department of Radiation Protection, China Institute of Atomic Energy, Beijing 102413, China

2 Nuclear and Radiation Safety Center, Ministry of Environment Protection, Beijing 100082, China

3 Occupational Radiation Protection Unit, Radiation Safety and Monitoring Section, NSRW, IAEA, PO Box 100, 1400 Vienna, Austria

1 Introduction

Gas proportional counters or plastic scintillators have been used widely for decades to detect beta rays [1–4]. Recently, semiconductor detector arrays and GM tubes were introduced [5–7] in the measurement for beta surface contamination, and corresponding devices were developed and used in the projects of Radalert (USA) [8], INSPECTOR (USA) [9], RDS 200 (Finland) [10], and so on. However, all the detectors have relatively small sensitive areas, in tens of cm^2 in maximum. For the measurement of whole body or large contaminated area, the main devices used for position-sensitive detection of beta ray are based on arrays of gas-flow proportional counters or plastic scintillators [3]. The position resolutions of these devices are generally about a few to tens of cm^2, determined by the sensitive area of a single detector in the array. Because of this, the detectors are not suitable for rapid measurement of surface contamination in the case of a nuclear emergency.

For several years, we have been studying a portable beta surface contamination monitor [11] based on large-area plastic scintillator and WLS fibers. It was found that increasing the sensitive detection area of the monitor could result in a series of problems, such as the reduction of detectable limit generated by increased system background and reduced optical collection efficiency, the inability to obtain accurate contamination distribution inside the sensitive detection area, and so on. In order to solve these problems, a new method for position-sensitive measurement of beta surface contamination was proposed, using large-area plastic scintillator and WLS fibers, and the "light center of gravity" method. The position of beta contamination could be determined based on the rules of light transmission, by recording the average amplitudes of output pulses from the two parallel WLS fibers of each fiber layer.

2 Materials and methods

2.1 Theoretical analysis on optical transmission

Plastic scintillator is widely used in radiation detection, and to improve the detection efficiency, large-size detectors are usually used [12–14]. According to theoretical and experimental studies on fluorescence photons transmission in large plate-shaped plastic scintillators in the past decade [15–22], the optical transmission follows the rules as below:

1. The photons caused by the interaction of beta ray with plastic scintillator are distributed evenly around the interaction point within the plastic scintillator.
2. The attenuation of photons in a plastic scintillator has an exponential relationship with the propagation distance, that is, the number of photons that can be collected depends on the distance between light collection device and the incident point.
3. For a relatively thin plastic scintillator, most of the fluorescent photons generated will be shot from the scintillator edge even in the absence of reflector. By adding the top and bottom surface reflector or improving the reflectivity of surface reflectors, the ratio of photons leaving from the edge will increase.
4. For a plastic scintillator of a certain size, an appropriate collection way can be designed to ensure that the number of photons collected by photosensitive components will not be affected by their distances from the incident location of the ray.

Therefore, for a determined detector structure and a uniformly emitting source, there is a correlation between the number of photons collected by light collection devices at different positions and device-source distances. So, we shall be able to determine the center of gravity of the light source (also the geometric center of beta-ray incident positions here) according to the signal intensities produced by light collection devices located at different distances.

2.2 Structure design of the detector

By fully referring to previous studies on the rules of fluorescence photons transmission in plastic scintillator, the collection capabilities of WLS fibers [23–27] and the method to connect fibers with scintillator [28–32], a position-sensitive detector for beta contamination using the "light center of gravity" method is designed, as shown schematically in Fig. 1.

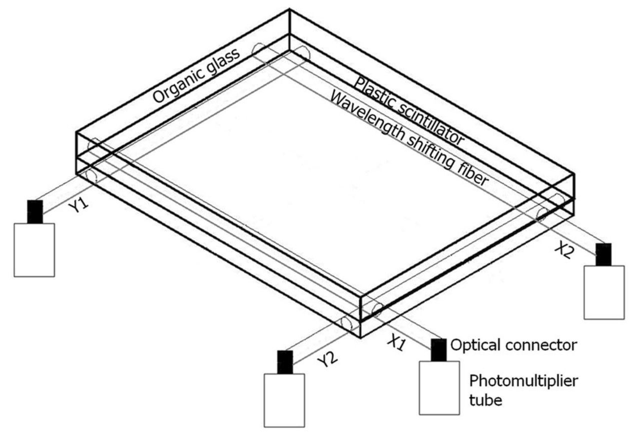

Fig. 1 A schematic diagram of the detector structure

The detector consists of a large-area plastic scintillator, WLS fibers, and organic glass. The WLS fiber has an inner core of Φ1 mm and cladding materials of 0.15 mm in thickness. The plastic scintillators were size at 40 cm × 30 cm, but the design was changed to 37 cm × 30 cm, considering that a greater distance between the two parallel WLS fibers would weaken efficiencies of light collection and coincidence measurement (see the simulation results in Sect. 3.1). They are 1.5 mm thick, determined according to the fiber diameter and influence of the scintillator thickness on the beta/gamma sensitivity [33]. Organic glass of 5 mm thickness is used for structural support and light transmission. Aluminum foil of about 2 mg/cm^3 mass thickness is used on the lower surface to shield and reflect light. In addition, to increase the optical collection efficiency as much as possible, a piece of reflection glass used as a reflector is installed on upper surface of the organic glass and around the composite structure. All optical interfaces are polished and applied with silicone oil.

In theory, because of different distances between the beta-ray incident points and the two parallel WLS fibers in the same fiber layer, the numbers of fluorescence photons collected by the two parallel WLS fibers are different (i.e., the corresponding amplitudes of output pulses generated after the PMT photoelectric conversion are different). Therefore, the incident position can be determined by analyzing the differences of output pulse amplitudes.

2.3 Simulation and optimization analysis

The detector structure was simulated with Geant4 toolkit to verify feasibility of the detection method and analyze position resolution of the detector. The bottom view from lower surface of the simulation model is shown in Fig. 2a. The sectional drawing perpendicular to the X axis is shown in Fig. 2b, in which Fibers Y1 and Y2 are fully embedded

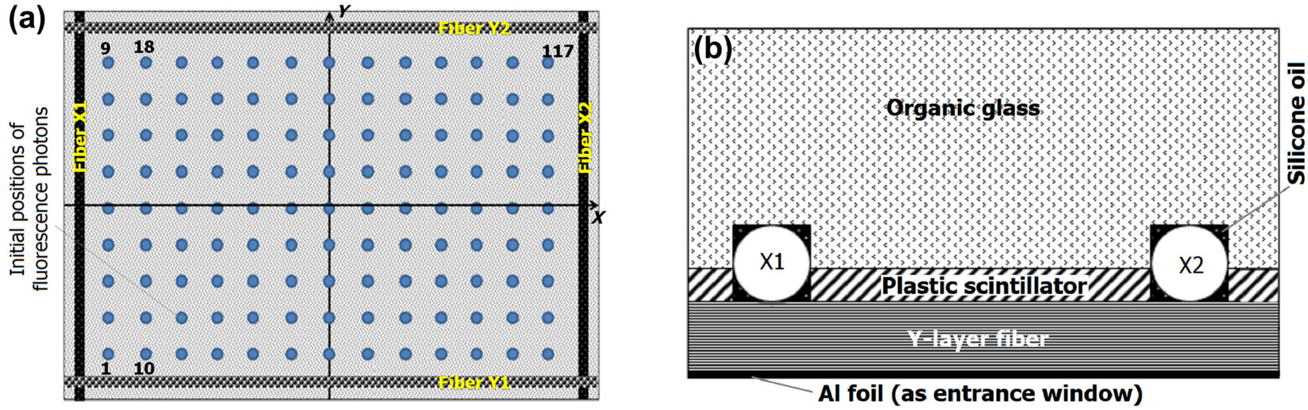

Fig. 2 Bottom view from lower surface of the simulation model (**a**) and structure model (*side view*) of the detector (**b**) in the simulation

in the scintillator, while X1 and X2 are embedded half in the scintillator and half in the organic glass.

To analyze the relationship between the number of photons emitted from the end faces of WLS fibers and the location of beta source, a series of initial (x, y) positions of fluorescence photon emission were specified as indicated in Fig. 2a, and the photons were collected and counted when they reached the end faces of WLS fiber.

It was assumed that the photons were homogeneously and isotropically distributed, and the center depth of photon emission is 0.75 mm. The refraction indexes of organic glass and silicone oil were, respectively, 1.49 and 1.53, and the refractivity of mirror glass around the plastic scintillator was 0.99. The refraction indexes of the inner core and the cladding materials of WLS fiber were, respectively, 1.68 and 1.49. The optical attenuation time of the fiber was about 2.7 s, and the light absorption length was over 3.5 m. The ranges of absorption and emission wavelengths of the fiber were, respectively, 350–475 and 460–600 nm, and the central absorption wavelength and central emission wavelength were, respectively, 435 and 490 nm.

The optical physical processes added in this work included G4Cerenkov, G4Scintillation, G4OpAbsorption, G4RayleighScattering, G4OpBoundaryProcess, and G4OpWLS. In order to improve the simulation accuracy, the number of incident photons sampled randomly at each incident location was 10,000, higher than the actual quantity produced during the interaction process of beta ray and the plastic scintillator.

2.4 Experiment system

Based on the simulation results, an experiment system for position-sensitive measurement of beta contamination was built to test and verify feasibility of the method and validity of the data acquisition and processing system. The overall scheme of the experiment system is shown in Fig. 3.

The experiment system was composed of four parts:

1. position-sensitive detector, which was implemented as the structure described above;
2. photoelectric conversion device, which was a CR110 photomultiplier tube (PMT) from Beijing Hamamatsu Company;
3. electronics system, which consisted of low-voltage power supply 4001C, pre-amplifier 142A, linear amplifier 572, 8-channel discriminator CF8000, 4-input logic unit CO4020 (all of the types above were produced by ORTEC from USA) and programmable high-voltage power supply N1471 produced by CAEN from Italy;
4. data acquisition system, which consisted of a computer and a data acquisition card PCI-9812 produced by D-Link Company. Output signal from the logic unit was used as the trigger signal to the data acquisition card.

2.5 Experiment methods

In the experimental measurement, in order to eliminate the strongly random interfering noises such as those from PMT and only the signals from the WLS fibers kept, a coincidence measurement method was adopted, as shown in Fig. 3.

In order to ensure the accuracy, a thin sheet with the incident points marked on was laid on the beta-ray incident surface of the plastic scintillator. The spacing of the incident points shown in Fig. 2a was about 3 cm. The beta source used was about 5 mm in diameter, and its geometric center was about 1 cm away from the surface of the plastic scintillator. When the beta source was located at an incident point, the output signal amplitudes from each WLS fiber were measured separately. The acquisition time for each incident point was 10 min, and the sampling frequency for each pulse was 8 times per second.

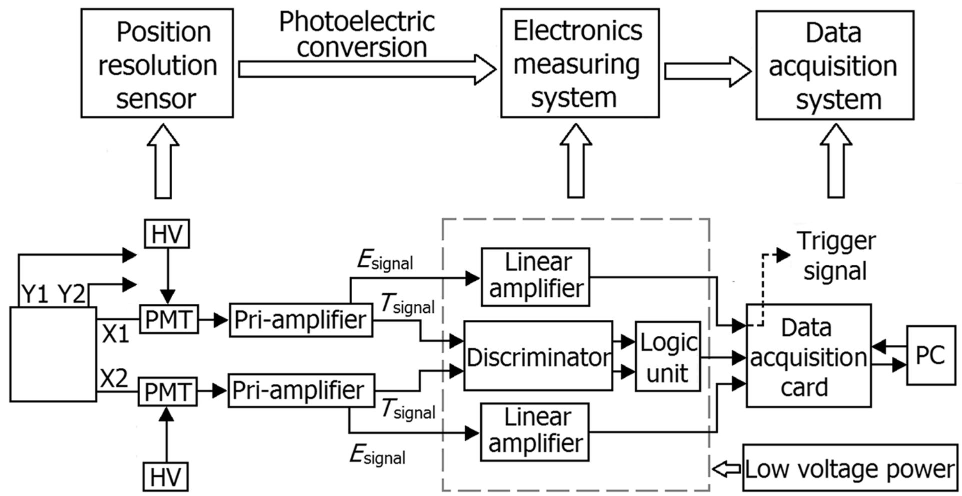

Fig. 3 Overall scheme of the experiment system

3 Results

3.1 Simulation results

The number of output photons from each WLS fiber was calculated at different incident positions, and the output photon were numbers averaged for all incident points at the same distance to the corresponding WLS fiber, by row or column. The data were fitted to obtain the relationship between the average number of output photons emitted from each WLS fiber and the distance from the incident point to the corresponding WLS fiber, as shown in Fig. 4.

A comparison was performed to obtain the ratio of output photon numbers from the two parallel WLS fibers in one (X or Y) fiber layer when the beta source was located at the different incident positions. Similar trends could be found in the results for X or Y fiber layer. The results for Y fiber layer are shown in Table 1.

To verify the accuracy of data processing by this method, polynomial fitting was used to obtain the relationship between the average ratio of output photon numbers from the two parallel WLS fibers in X or Y fiber layer and the incident position-fiber distance. Figure 5 shows the results for X and Y fiber layers.

3.2 Experiment results

As shown in Fig. 6, evidences from two aspects proved effectiveness of the experiment data. Firstly, the pulse signals had the source correlation properties after using the coincidence method. Secondly, the amplitude spectrum of output pulses from the fibers was shaped almost the same

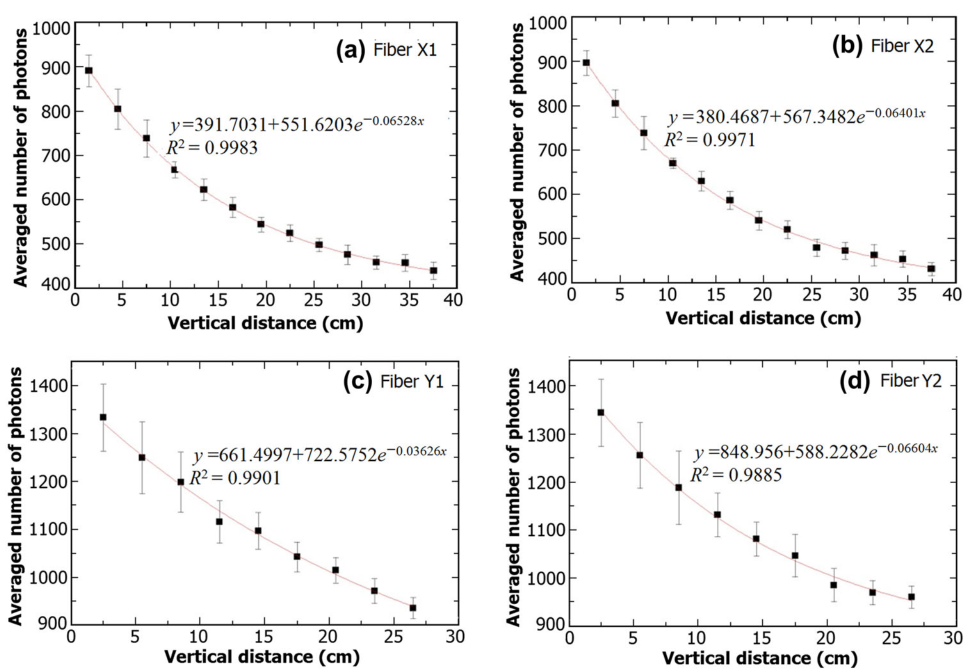

Fig. 4 Number of the output photons from each fiber as a function of the incident position

Table 1 Ratio of the output photon numbers from the two parallel WLS fibers in Y fiber layer at different beta-ray incident positions (Y1/Y2)

Vertical distance to Y1 (cm)	Ratios (Y1/Y2) for the incident positions with the different vertical distances (cm) to X1 fiber													
	1.5	4.5	7.5	10.5	13.5	16.5	19.5	22.5	25.5	28.5	31.5	34.5	37.5	Average
2.5	1.237	1.410	1.414	1.480	1.371	1.427	1.445	1.441	1.464	1.370	1.408	1.355	1.263	1.391
5.5	1.161	1.224	1.250	1.400	1.364	1.380	1.279	1.362	1.328	1.351	1.291	1.181	1.211	1.291
8.5	1.151	1.124	1.311	1.212	1.253	1.266	1.305	1.274	1.244	1.170	1.120	1.198	1.219	1.219
11.5	1.038	1.122	1.031	0.992	1.122	1.080	1.075	1.088	1.127	1.103	1.009	1.061	1.043	1.068
14.5	1.023	1.037	0.972	0.962	1.012	1.004	0.982	1.020	1.097	1.022	1.023	0.961	1.098	1.016
17.5	0.880	0.937	0.859	0.941	0.964	0.906	0.882	0.894	0.926	0.929	0.919	0.994	0.962	0.923
20.5	0.861	0.908	0.892	0.869	0.821	0.819	0.786	0.796	0.800	0.886	0.935	0.822	0.950	0.857
23.5	0.831	0.798	0.766	0.723	0.784	0.753	0.740	0.713	0.719	0.781	0.798	0.783	0.897	0.776
26.5	0.758	0.685	0.713	0.651	0.691	0.655	0.657	0.723	0.695	0.668	0.723	0.695	0.748	0.697

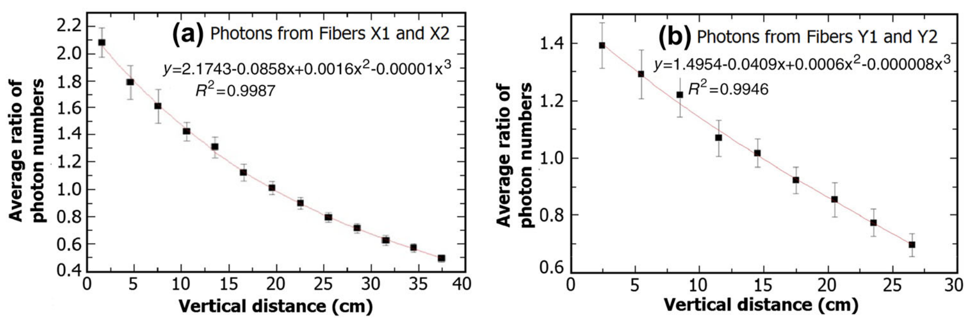

Fig. 5 Average ratio of output photon numbers from the two parallel WLS fibers plotted as a function of incident position

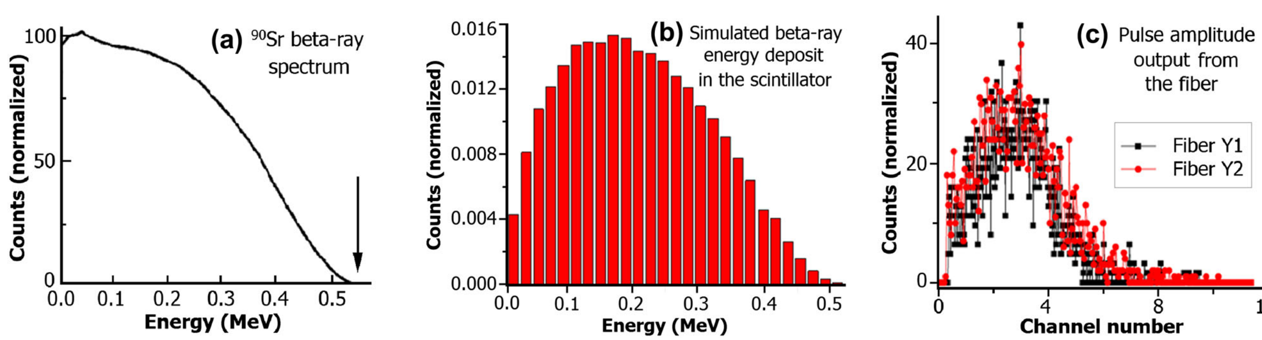

Fig. 6 Comparison of the energy spectra

as the beta-ray energy spectrum emitted from the ^{90}Sr source and the simulated spectrum for ^{90}Sr beta-ray energy deposit in the scintillator.

As the signal processing system was independently used for each fiber, inconsistency of photoelectric conversion could be introduced. Theoretically, when the beta source was located at incident positions with the same distance to the two parallel WLS fibers in X or Y fiber layer, the average amplitudes of output signals from the two fibers should be equal. Therefore, a correction factor could be obtained to equalize the average output amplitudes from the two parallel fibers, so as to correct the inconsistency of the photoelectric conversion.

For each WLS fiber, the average amplitude of output pulses from the fiber was taken with the beta source being at different incident positions in the same distances to the fiber. By fitting the data, the relationship between the average amplitude of output pulses from each WLS fiber and the incident point-fiber distance could be obtained, as shown in Fig. 7.

Then, by comparing the ratios of average pulse amplitudes output from the two parallel WLS fibers in X or Y fiber layer with the beta source being at the different incident positions, the data showed similar trends to the simulation results. The results for Y fiber layer are shown in Table 2.

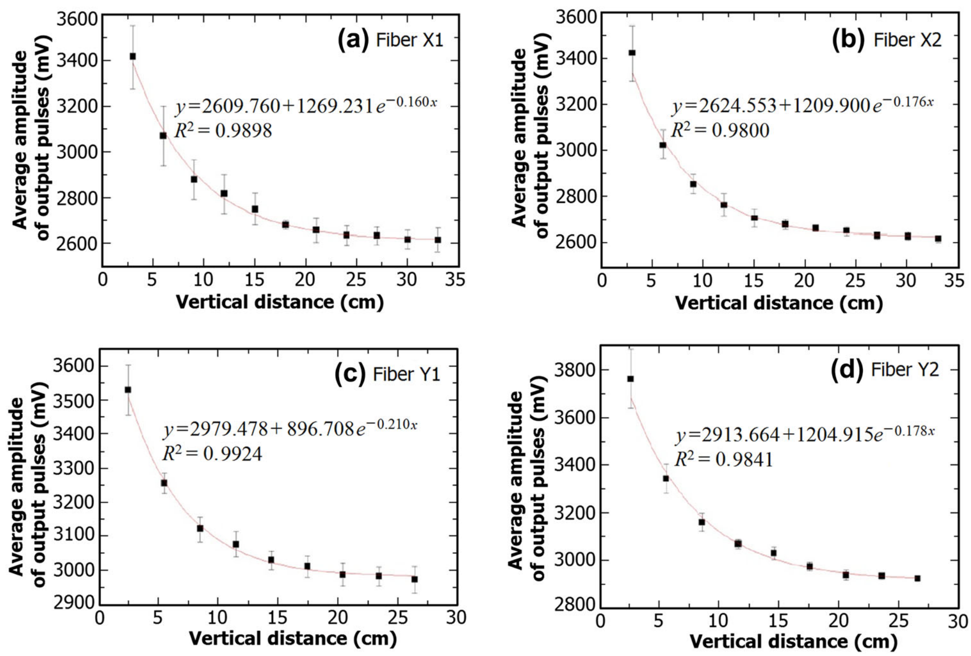

Fig. 7 Average amplitude of output pulse plotted as a function of incident position

Table 2 Ratio of the average pulse amplitudes output from the two parallel WLS fibers in Y fiber layer at different incident positions (Y1/Y2)

Vertical distance to Y1 (cm)	Ratio (Y1/Y2) for the incident positions with different vertical distances (cm) to X1 fiber											
	3	6	9	12	15	18	21	24	27	30	33	Average
2.5	1.233	1.228	1.180	1.187	1.176	1.208	1.199	1.188	1.206	1.241	1.242	1.208
5.5	1.100	1.128	1.106	1.111	1.108	1.102	1.097	1.094	1.112	1.124	1.129	1.110
8.5	1.045	1.079	1.063	1.056	1.070	1.064	1.062	1.054	1.051	1.082	1.062	1.062
11.5	1.035	1.060	1.039	1.030	1.043	1.044	1.023	1.036	1.020	1.030	1.020	1.035
14.5	1.000	1.000	1.000	1.000	1.000	1.000	1.000	1.000	1.000	1.000	1.000	1.000
17.5	0.971	0.989	0.981	0.993	1.004	0.987	0.969	0.983	0.962	0.987	0.970	0.981
20.5	0.930	0.938	0.942	0.944	0.952	0.958	0.945	0.950	0.947	0.947	0.946	0.945
23.5	0.897	0.878	0.880	0.886	0.903	0.893	0.867	0.931	0.878	0.916	0.882	0.892
26.5	0.768	0.759	0.755	0.811	0.807	0.832	0.783	0.822	0.804	0.773	0.780	0.790

The relationships between the average ratio of output pulse amplitudes from the two parallel WLS fibers in X or Y fiber layer and the incident position-fiber distance are shown in Fig. 8.

4 Discussions

4.1 Analysis of simulation results

When the beta source is located at different incident points in the same distance to the corresponding WLS fiber, the numbers of output photons emitted from the fiber are almost the same, and the photon numbers decrease with increasing vertical distance to the fiber.

When the beta source is located at different rows or columns of the grid, the average number of output photons from each WLS fiber is an exponential function of the source-fiber distance,

$$y = y_0 + A\exp(R_0 x), \tag{1}$$

where y is the average photon number output from the fiber, x is vertical distance from the source position to the fiber, and y_0 and R_0 are constants. R_0, in unit of centimeter, is negative reciprocal of the effective attenuation coefficient of photon transmission in the scintillator, also known as the fluorescence decay length of scintillator [34] (under certain conditions it is also known as the technical light attenuation length).

The results are consistent to the light transmission rules in the scintillator, with correlation coefficients of over 0.99.

Fig. 8 Average ratio of the output pulse amplitudes plotted as a function of incident position

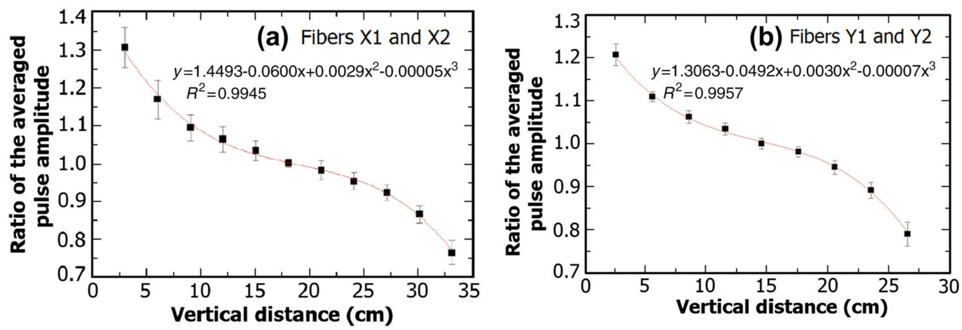

It indirectly proves the feasibility of embedding WLS fiber into the scintillator to improve the light collection.

When the beta source is located at different rows or columns of the grid, the average ratio of output photon numbers from the two parallel WLS fibers in X or Y fiber layer is a third-order polynomial function of the source-fiber distance,

$$y = B_0 + B_1x + B_2x^2 + B_3x^3, \quad (2)$$

where y is the average ratio of output photon numbers from the two parallel WLS fibers in the same fiber layer; x is vertical distance from one of the two WLS fibers to the incident positions of beta ray; and B_0, B_1, B_2, and B_3 are constants.

4.2 Analysis of experiment results

As a whole, the experiment results agree well with the simulation results in the curve shape, while the constant values obtained by fitting are different.

For a single WLS fiber, the R_0 values obtained from the experiment are about 0.2 cm^{-1}, significantly higher than the simulation results (about 0.06 cm^{-1}). This indicates a large gap between the actual light coupling effect and the model used in the simulation, though the scintillators are roughly of the same size and shape. So the layout of reflector and the light coupling process remain to be further improved.

For each WLS fiber layer, when the beta source is at different incident points over the scintillator surface, there is also a polynomial relationship between the average ratio of output pulse amplitudes from the two parallel WLS fibers and the beta-ray incident point-fiber distance.

To sum up, the incident position of the beta ray can be determined by measuring the average amplitude ratio of the output pulses with the position-sensitive detector calibrated.

5 Conclusion

In this paper, optical characteristics are explained for a position-sensitive detector based on a large-area plastic scintillator and WLS fibers. The detector has the position resolution ability to beta rays, and the measurement method is effective.

However, for surface contamination measurement with the current design, the detector uniformity shall be improved and the detection efficiency is relatively low, due to mainly the unsatisfactory light coupling and small technical light attenuation length. For higher measurement precision, we will focus on (1) improving optical coupling toward greater light collection efficiency and detector uniformity, and (2) increasing the number of WLS fibers, that is, to reduce the size of WLS fiber grid, toward larger technical light attenuation length of the detector and greater light collection efficiency.

In addition, the position-sensitive detector designed in this work is in similar size to the previous measuring device of beta radioactivity. However, by using the coincidence measurement method, the noise level of present position-sensitive detector can be reduced significantly to about 150/min, rather than about 2000/min of previous radioactivity-measuring device. Then the detector's background shall be correspondingly reduced with this improvement. Besides, the efficiency of light collection can be significantly improved by increasing the density of fiber grid. Since the minimum detectable limit of the detector mainly depends on the background level and detection efficiency, it is possible to achieve lower minimum detectable limit of the position-sensitive detector than previous radioactivity-measuring device, with the improvements of both background level and detection efficiency.

Acknowledgements We express our gratitude to Prof. Xiang-Cheng Meng with Institute of High Energy Physics and Prof. Cheng-Jian Lin with China Institute of Atomic Energy for their encouragement, information, and discussion.

References

1. S.O. Troja, A. Cro, P. Picouet, Alpha and beta dose-rate determination using a gas proportional counter. Radiat. Meas. **24**, 297–308 (1995). doi:10.1016/1350-4487(94)00110-M
2. D. Stanga, J.L. Picolo, N. Coursol et al., Analytical calculations of counting losses in internal gas proportional counting. Appl.

Radiat. Isotopes. **56**, 231–236 (2002). doi:10.1016/S0969-8043(01)00193-2

3. W.A. Fisher, J.W. Wanless, Effect of elevated backgrounds on plastic scintillator based whole body contamination monitors. IEEE. T. Nucl. Sci. **34**, 606–610 (1987). doi:10.1109/TNS.1987.4337416
4. L. Miramonti, A plastic scintillator detector for beta particles. Radiat. Meas. **35**, 347–354 (2002). doi:10.1016/S1350-4487(02)00051-3
5. E.B. Farfán, S.P. Gaschak, A.M. Maksymenko et al., Assessment of beta particle flux from surface contamination as a relative indicator for radionuclide distribution on external surfaces of a multistory building in Pripyat. Health Phys. **100**, 221–227 (2011). doi:10.1097/HP.0b013e3181ee31ac
6. S. Grujić, I. Đorđević, M. Milošević et al., Monte carlo simulation of GM probe and NaI detector efficiency for surface activity measurements. Radiat. Meas. **58**, 45–51 (2013). doi:10.1016/j.radmeas.2013.08.002
7. S. Grujić, M. Milošević, U. Kozmidis-Luburić et al., Monte carlo simulation of beta radiation response function for semiconductor Si detector. Nucl. Instrum. Meth. A. **654**, 288–292 (2011). doi:10.1016/j.nima.2011.06.070
8. O.A. Gregory, U.N. Felix, E.E. Oghenevovwero, Assessment of background ionization radiation of oil spillage site at Obodo Creek in Gokana L.G.A. of River State. Nigeria. Brit. J. Appl. Sci. Tech. **4**, 5072–5079 (2014). doi:10.9734/BJAST/2014/12502
9. R. Owen, K. Drummond, K. Viverito et al., Monitoring and managing metabolic effects of antipsychotics: a cluster randomized trial of an intervention combining evidence-based quality improvement and external facilitation. Implement. Sci. **8**, 1–12 (2013). doi:10.1186/1748-5908-8-120
10. O.D. Oyeyinka, I.U. James, E.C. Akueche et al., Estimation of radiation dose rate levels around a nuclear establishment in Abuja, North Central. Nigeria. Sci. Technology. **2**, 163–167 (2012). doi:10.5923/j.scit.20120206.04
11. Y.T. Qu, J. Hou, Y. Liu et al., Performance test and analysis to the prototype of fiber-based portable large area surface contamination monitor. Radiat. Prot. (in Chinese) **33**, 334–339 (2013)
12. J. Nilsson, M. Isaksson, A comparison between Monte Carlo-calculated and -measured total efficiencies and energy resolution for large plastic scintillators used in whole-body counting. Radiat. Prot. Dosim. **144**, 555–559 (2011). doi:10.1093/rpd/ncq340
13. P.C. Rout, D.R. Chakrabarty, V.M. Datar et al., A large area plastic scintillator detector array for fast neutron measurements. Nucl. Instrum. Meth. A. **598**, 526–533 (2009). doi:10.1016/j.nima.2008.09.034
14. W. Bugg, Yu. Efremenko, S. Vasilyev, Large plastic scintillator panels with WLS fiber readout: optimization of components. Nucl. Instrum. Meth. A. **758**, 91–96 (2014). doi:10.1016/j.nima.2014.05.055
15. L. Chen, X.P. Ouyang, Z.B. Zhang et al., Study on luminescence intensity space distribution of film scintillator. Chin. J. Nucl. Sci. Eng. (in Chinese) **27**, 317–321 (2007). doi:10.3321/j.issn:0258-0918.2007.04.005
16. L. Fan, Y.G. Li, J.F. Ji, A study of photons collection in plastic scintillation. Nucl. Electron. Detect. Technol. (in Chinese) **23**, 117–120 (2003). doi:10.3969/j.issn.0258-0934.2003.02.006
17. V. Senchyshyn, V. Lebedev, A. Adadurov et al., Accounting for self-absorption in calculation of light collection in plastic scintillators. Nucl. Instrum. Meth. A. **566**, 286–293 (2006). doi:10.1016/j.nima.2006.06.037
18. S. Scheu, H. Kaspar, P. Robmann et al., Studies on wrapping materials and light collection geometries in plastic scintillators. Nucl. Instrum. Meth. A. **567**, 345–349 (2006). doi:10.1016/j.nima.2006.05.153
19. Y.L. Li, Y.J. Li, L.B. Xu et al., Study on the light transport in long and narrow scintillators. Nucl Electron Detect Technol. **23**, 534–537 (2003). doi:10.3969/j.issn.0258-0934.2003.06.011. **(in Chinese)**
20. L. Cao, W. Kang, C.S. Chu et al., A study of large area rectangular plastic scintillator for detecting γ with high detection efficiency. Nucl. Electron. Detect. Technol. (in Chinese) **29**, 52–54 (2009). doi:10.3969/j.issn.0258-0934.2009.01.013
21. L. Bläckberg, M. Klintenberg, A. Ringbom et al., Effects of surface coatings on the light collection in plastic scintillators used for radioxenon detection. Phys. Scripta. **150**, 963–967 (2012). doi:10.1088/0031-8949/2012/T150/014007
22. T. Mizuno, Y. Kanai, J. Kataoka et al., A Monte Carlo method for calculating the energy response of plastic scintillators to polarized photons below 100 keV. Nucl. Instrum. Meth. A. **600**, 609–617 (2009). doi:10.1016/j.nima.2008.11.148
23. F. Nishikido, T. Moritake, S. Kishimoto et al., X-ray detector made of plastic scintillators and WLS fiber for real-time dose distribution monitoring in interventional radiology, in *Nuclear Science Symposium and Medical Imaging Conference (NSS/MIC), 2012 IEEE* (2012), pp. 1272–1274. doi:10.1109/NSSMIC.2012.6551311
24. H.N. Du, Y.F. Yang, S.R. Cherry, Comparison of four depth-encoding PET detector modules with wavelength shifting (WLS) and optical fiber read-out. Phys. Med. Biol. **53**, 1829–1842 (2008). doi:10.1088/0031-9155/53/7/002
25. M. Itaya, T. Inagaki, T. Iwata et al., Development of a new photomultiplier tube with high sensitivity for a wavelength-shifter fiber readout. Nucl. Instrum. Meth. A. **522**, 477–486 (2004). doi:10.1016/j.nima.2003.11.201
26. Y. Ito, G. Katano, H. Harano et al., Development of a tiny neutron probe with an optical fiber for BNCT. Radiat. Prot. Dosim. **110**, 619–622 (2004). doi:10.1093/rpd/nch136
27. M.L. Crow, J.P. Hodges, R.G. Cooper, Shifting scintillator prototype large pixel wavelength-shifting fiber detector for the POWGEN3 powder diffractometer. Nucl. Instrum. Meth. A. **529**, 287–292 (2004). doi:10.1016/j.nima.2004.04.167
28. O. Mineev, Y. Kudenko, Y. Musienko et al., Scintillator detectors with long WLS fibers and multi-pixel photodiodes. J. Instrum. **6**, 12004 (2011). doi:10.1088/1748-0221/6/12/P12004
29. M. Kubo, H. Kawai, Y. Kishi et al., Development of the new silica aerogel Cherenkov counter using WLS fiber and MPPC, in *Nuclear Science Symposium and Medical Imaging Conference (NSS/MIC), 2011 IEEE* (2011), pp. 1103–1106. doi:10.1109/NSSMIC.2011.6154581
30. A.K. Jones, D. Hintenlang, Potential clinical utility of a fiber optic-coupled dosimeter for dose measurements in diagnostic radiology. Radiat. Prot. Dosim. **132**, 80–87 (2008). doi:10.1093/rpd/ncn252
31. A.M.C. Santos, M. Mohammadi, S. Afshar, Optimal light collection from diffuse sources: application to optical fiber-coupled luminescence dosimetry. Opt. Express **22**, 4559–4574 (2014). doi:10.1364/OE.22.004559
32. L.A. Benevides, A.L. Huston, B.L. Justus et al., Characterization of a fiber-optic-coupled radioluminescent detector for application in the mammography energy range. Med. Phys. **34**, 2220–2227 (2007). doi:10.1118/1.2736788
33. T. Maekawa, A. Sumita, S. Makino et al., Thin beta-ray detectors using plastic scintillator combined with wavelength-shifting fibers for surface contamination monitoring. J. Nucl. Sci. Technol. **35**, 886–894 (1998). doi:10.1080/18811248.1998.9733961
34. I. Vilardi, A. Braem, E. Chesi et al., Optimization of the effective light attenuation length of YAP: Ce and LYSO: Ce crystals for a novel geometrical PET concept. Nucl. Instrum. Meth. A. **564**, 506–514 (2006). doi:10.1016/j.nima.2006.04.079